2007 SCEC Annual Report: Resolution of Kinematic Source Models
Principal Investigator: Jean M. Carlson
Institution: UC Santa Barbara

A. Resolution of GPS Data from the 2004 M6.0 Parkfield Earthquake

Given a linear inverse problem, the resolution matrix $R=G^{-g}G$ is a function of the Green's function G and the generalized inverse G^{-g}. If the inversion has perfect resolution, the resolution matrix will equal the identity matrix. In practice, the rows of R give weighted averages of the model parameters [*Menke*, 1989]. The extent to which the weights along the diagonal elements of R "leak" into neighboring elements in each row gives a measure of the resolution of each model parameter.

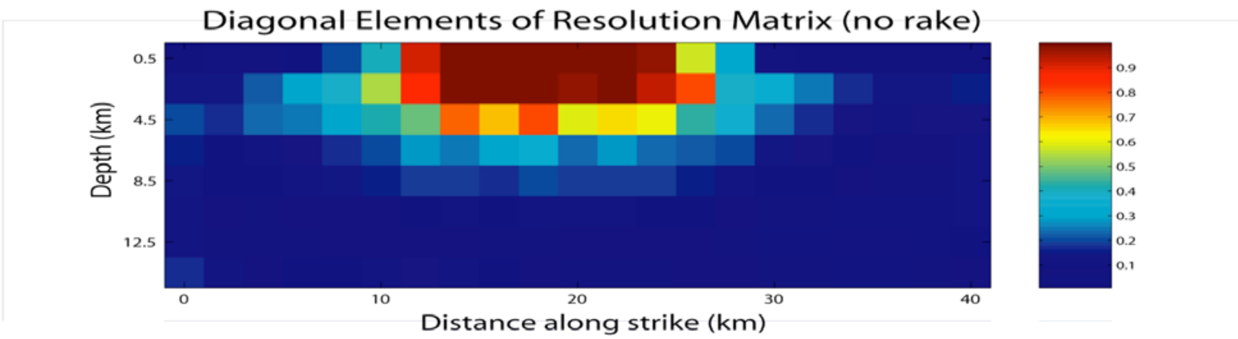

Figure 1. Diagonal elements of the resolution matrix for the GPS data from the 2004 Mw6.0 Parkfield Earthquake plotted on their corresponding subfaults. Resolution is poor at depth and near the edges of the fault.

We found that even for a well-recorded earthquake such as the 2004 M6.0 Parkfield earthquake, which was recorded by 13 near-field GPS stations, static GPS inversions are poorly resolved at depth and near the edges of the fault. Figure 1 shows the on-diagonal elements of the resolution matrix mapped onto the fault plane. In poorly resolved areas of the fault, slip is poorly constrained spatially, which can lead to artifacts at depth. The location of these artifacts, which often look very similar to asperities, is a function of the station locations and velocity structure.

B. Inversion of Parkfield GPS Data

Formulating the inverse problem in a way that is severely underdetermined can lead to spurious structure in the final model. In the inversion of Parkfield GPS data, the resolution is highly spatially variable, with a much smaller resolution length near the top and center of the fault plane. We can improve the model resolution by making the subfaults larger in poorly resolved areas. A nonuniform grid with subfaults (grid cells) that match the local resolution length on the fault plane simultaneously maximizes the recoverable information in well-resolved areas of the fault while avoiding spurious structure in poorly resolved areas.

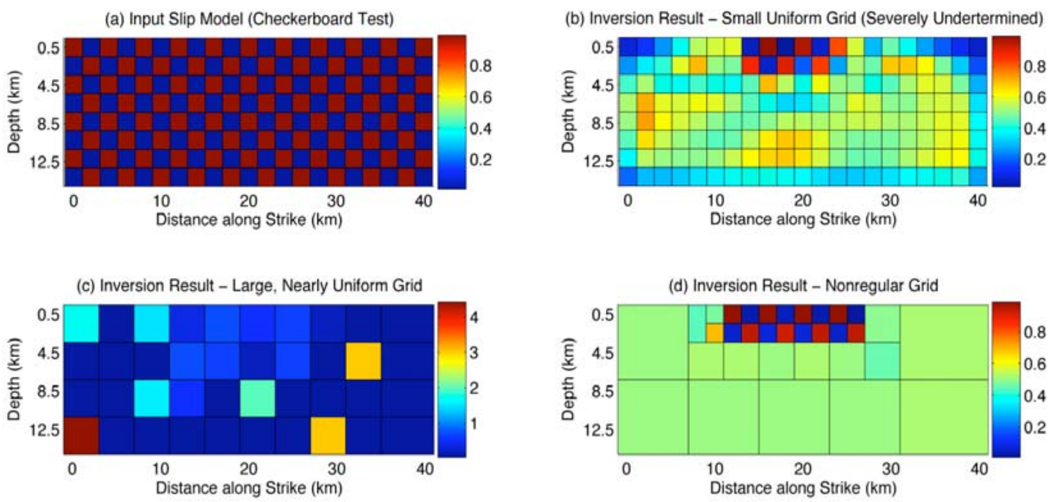

Figure 2. We generated data from a synthetic slip model (a checkerboard test) shown in (a) and inverted the data onto three different grids. b) With a small, uniform grid, spurious structure is generated at depth. c) With a larger uniform gridding, structure near the surface is lost and spurious structure is again generated at depth in part because the large subfaults near the surface are removing structure that is within the resolution length of the problem. d) With a nonuniform grid with spacing that approximates the local resolution length on the fault plane, structure is adequately recovered in well-resolved portions of the fault and spurious slip is avoided in poorly resolved areas.

We performed a traditional inversion of the Parkfield GPS data on a uniform grid and compared this result to an inversion performed on the nonuniform grid shown in Figure 2d. Figures 3a and 3b show the slip model from the uniform-grid inversion and the associated perturbation error from a Monte Carlo sampling of the errors in the GPS data. The inversion on the nonuniform grid, as shown in Figure 3c, captures the resolution error in the gridding of the fault plane. In our view, the nonuniform-grid inversion of the Parkfield GPS data is superior because it assesses both resolution and perturbation errors. In addition, it is less likely to contain artifacts because the larger subfaults at depth limit the number of free parameters.

C. Two-Step Inversion with Strong-Motion Data

We constrained the final slip in an inversion of strong-motion data to match the final slip given by the GPS data, within the error bounds. The GPS inversion of the regular grid does not place enough slip near the hypocenter to satisfy strong-motion stations to the southeast. One might think that this suggests an inconsistency between the GPS and strong-motion data, but in fact the GPS inversion on the irregular grid is consistent with the strong motion data. The non-uniform grid allows us to capture resolution error, and when this is taken into account, the two datasets agree. This confirms our view that the nonuniform grid produces more reliable results with fewer artifacts.

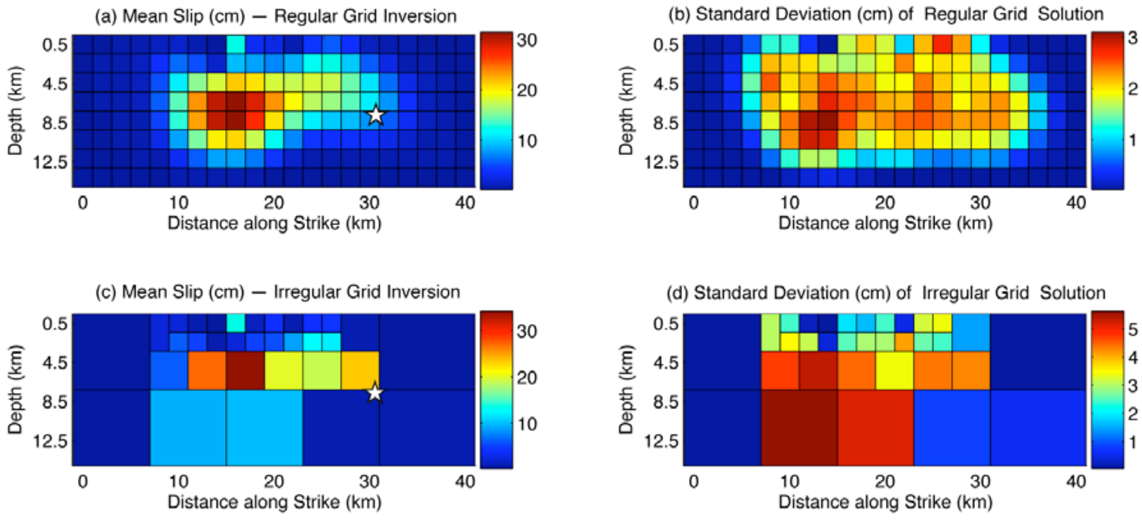

Figure 3. Inversion of Parkfield GPS data on a regular grid (a), and on an irregular grid (c), with associated perturbation errors found via Monte Carlo sampling of GPS errors (b and d). Both inversions give similar fits to the data with a variance reduction of 89-90%.

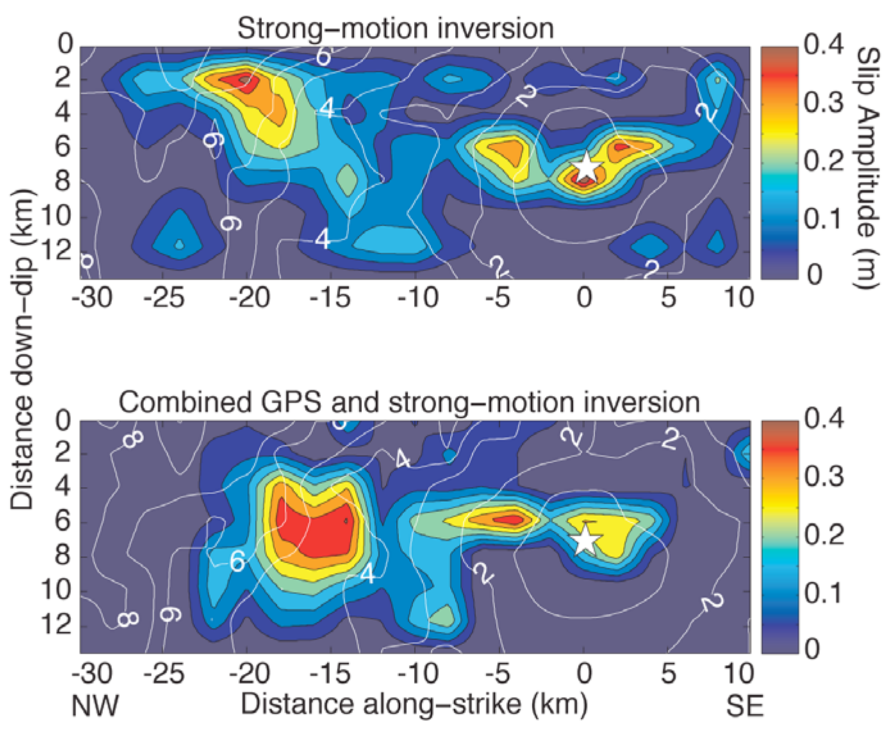

Figure 4. Inversion of strong-motion GPS data without any static-field constraint [*Liu et al.*, 2006] (a), and with the addition of a final-slip constraint derived from the GPS data inverted on a nonuniform grid (b). The addition of GPS data results in a more compact final slip distribution.

D. Resolution of Strong-Motion Data

Strong-motion data has the ability to see slip deeper than static data because the static field decays faster with source-to-receiver distance [*Aki and Richards*, 2002]. Synthetic tests of different data types confirm this (e.g., [*Delouis et al.*, 2002]). However, strong-motion data is further complicated by rupture time, which adds a strong nonlinearity to the inverse problem. We linearized the strong-motion inversion about the fiinal rupture times determined by a nonlinear simulated annealing algorithm in order to investigate the resolution and covariance of the model.

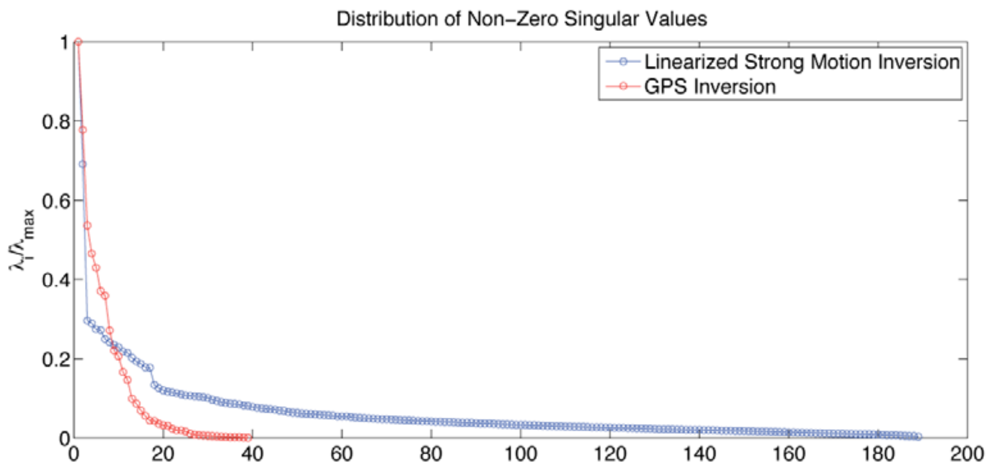

Figure 5. Distribution of singular values for the GPS inversion (red) and for a linearized strong-motion inversion (blue). The strong-motion inversion is not technically underdetermined, although many of the singular values are near zero, which means some slip vectors are unstable.

Model vectors that correspond to small singular values are unstable to data perturbations. In Figure 5 we plot the distribution of singular values for the GPS inversion and for the linearized strong-motion inversion. Even though this linearized version of the strong-motion inversion is overdetermined, many of the model parameters (particularly at depth) are unstable, and thus very sensitive to data perturbations.

The log of the model covariance matrix, shown in Figure 6, shows that parameters at depth are far more sensitive to data perturbations than shallower parameters. This is important because a major source of perturbation error in strong-motion inversions is due to Green's function errors. Strong-motion inversions of the dynamic wavefield are more sensitive to the velocity structure than are static inversions [*Wald and Graves,* 2001]. Errors in the Green's function due to incorrect velocity structure or fault location are highly nonlinear, and can change the final slip model significantly [*Das and Suhadolc,* 1996; *Sekiguchi et al*., 2000]. A thorough quantification of errors in kinematic inversions will allow for the determination of robust features in the models, which will allow researchers to draw firmer conclusions from this information.

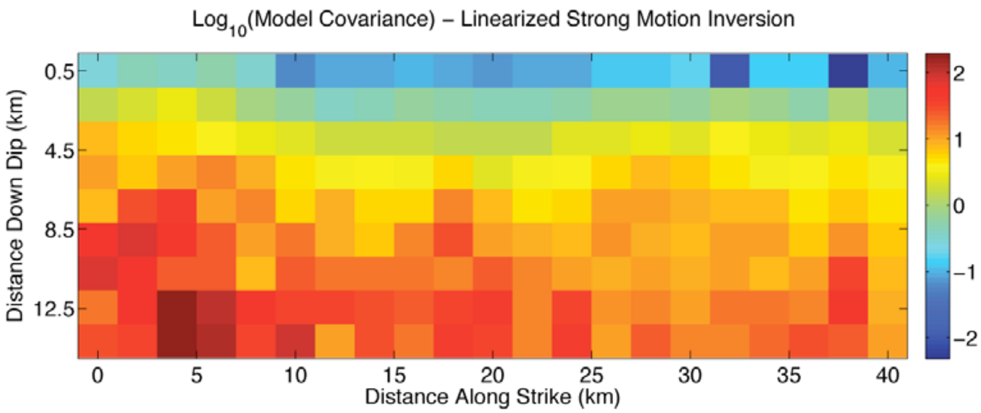

Figure 6. The model covariance, which shows how sensitive model parameters are to perturbations in the data, is shown plotted onto the fault plane for a linearized strong-motion inversion.

Publications:

Custódio, Susana, Morgan T. Page, Ralph J. Archuleta, and J.M. Carlson. Constraining Earthquake Source Inversions with GPS Data 2: A Two-Step Approach to Combine Seismic and Geodetic Datasets, submitted to J. Geophys. Res. - Solid Earth, SCEC contribution #1125.

Page, Morgan, Susana Custódio, Ralph J. Archuleta, and J. M. Carlson. Constraining Earthquake Source Inversions with GPS Data 1: Resolution Based Removal of Artifacts, submitted to J. Geophys. Res. - Solid Earth, SCEC contribution #1127.

Presentations:

Page, Morgan, Susana Custódio, Ralph J. Archuleta, and J. M. Carlson, Using resolution information to remove artifacts from GPS inversions, poster, American Geophysical Union Fall Meeting, 2007.

Page, Morgan, Susana Custódio, Ralph J. Archuleta, and J. M. Carlson, GPS inversions: What can they resolve?, invited talk, Dix Seismo Lab Seminar, California Institute of Technology, 2007.

Page, Morgan, Susana Custódio, Ralph J. Archuleta, and J. M. Carlson, Constraining earthquake source inversions with GPS data: Resolution based removal of artifacts, invited talk, U.S. Geological Survey, Menlo Park, 2007.

Page, Morgan, Susana Custódio, Ralph J. Archuleta, and J. M. Carlson, Using resolution information to eliminate artifacts in earthquake source inversions, invited talk, University of Southern California, 2007.

Page, Morgan, Susana Custódio, Ralph J. Archuleta, and J. M. Carlson, Resolution of GPS data from the 2004 M6.0 Parkfield earthquake, poster, Southern California Earthquake Center Annual Meeting, 2007.

Page, Morgan, Susana Custódio, Ralph J. Archuleta, and J. M. Carlson, Resolution of GPS data from the 2004 M6.0 Parkfield earthquake, poster, Seismological Society of America Annual Meeting, 2007.

Page, Morgan, Susana Custódio, Ralph J. Archuleta, and J. M. Carlson, Resolution of slip from Inversions of GPS data, Lamont-Doherty Earth Observatory, 2007.

References:

Aki, K., and P. G. Richards (2002), Quantitative Seismology, second ed., University Science, Sausalito, California.

Das, S., and P. Suhadolc (1996), On the inverse problem for earthquake rupture: The Haskell-type source mode, J. Geophys. Res., 101(B3), 5725–5738.

Delouis, B., D. Giardini, P. Lundgren, and J. Salichon (2002), Joint inversion of InSAR, GPS, teleseismic, and strong-motion data for the spatial and temporal distribution of earthquake slip: Application to the 1999 Izmit mainshock, Bull. Seismol. Soc. Am., 92(1), 278–299.

Liu, P., S. Custódio, and R. J. Archuleta (2006), Kinematic inversion of the 2004 M_w6.0 Parkfield earthquake including an approximation to site effects, *Bull. Seismol. Soc. Am.*, **96**, 4B, doi: 10.1785/0120050826

Menke, W. (1989), Geophysical Data Analysis: Discrete Inverse Theory, Academic Press, San Diego.

Sekiguchi, H., K. Irikura, and T. Iwata (2000), Fault geometry at the rupture termination of the 1995 Hyogo-ken Nanbu earthquake, Bull. Seismol. Soc. Am., 90(117-133), 117–133.

Wald, D. J., and R. W. Graves (2001), Resolution analysis of finite fault source inversion using one- and three-dimensional Green’s functions: 2. Combining seismic and geodetic data, J. Geophys. Res., 106(B5), 8767–8788.